

Modeling and Simulation of Hollow Fiber Modules of Hybrid Facilitated Transport Membranes for Flue Gas CO₂ Capture [†]

Abbos Elmanov ¹, Abdulaziz Bakhtiyorov ¹, Zafar Turakulov ^{1,2}, Azizbek Kamolov ^{1,2} and Adham Norkobilov ^{1,*}

¹ Shahrissabz Branch of the Tashkent Institute of Chemical Technology; abbos-ktishf@gmail.com (A.E.); email1@email.com (A.B.); email2@email.com (Z.T.); email3@email.com (A.K.)

² Tashkent Institute of Chemical Technology; webdastur@gmail.com (X.X.)

* Correspondence: adham.norkobilov@gmail.com; Tel.: +998-993015567

[†] Presented at the 2nd International Electronic Conference on Processes: Process Engineering—Current State and Future Trends (ECP 2023), 17–31 May 2023; Available online: <https://ecp2023.sciforum.net/>.

Abstract: The basis for modeling and simulation of the post-combustion CO₂ capture process has been developed using hollow fiber membrane technology. The membrane cell was modeled using Aspen Custom Modeler (ACM) and exported to Aspen Plus as a membrane unit. The Aspen Plus methodology has been effectively used to estimate the physico-chemical parameters of CO₂ absorption by kinetic and thermodynamic models. The membrane cell for the permeation of gas mixtures was programmed using ACM and successfully imported into the simulation media, as there was no model block included for the hollow fiber membrane unit in the standard package for a process flowsheet simulation. The transport mechanism in hollow fiber membranes has been discussed, and both empirical and theoretical models are presented for the facilitated transport theory of gases in membrane cells. The goal of modeling membrane cells is to design and optimize membranes for carbon capture processes. The concept of modeling membrane processes is identified, and some of the most important aspects of the simulation of membrane systems are discussed. As a reference, a CO₂ flux of more than 700 NL m⁻²h⁻¹ through a membrane cell was obtained. Challenges adversely affecting the separation performance of hollow fiber-based gas separation membranes are explained in detail, and the significance of incorporating the effects of such challenges into membrane models is clarified. Parameters affecting the separation performance of hollow fiber-based gas separation membranes have been studied, and the significance of integrating the effect of probable challenges into membrane models is clarified.

Keywords: carbon capture; modeling; hollow fiber; membrane; model; separation

Citation: Elmanov, A.; Bakhtiyorov, A.; Turakulov, Z.; Kamolov, A.; Norkobilov, A. Modeling and Simulation of Hollow Fiber Modules of Hybrid Facilitated Transport Membranes for Flue Gas CO₂ Capture. *Eng. Proc.* **2023**, *37*, x. <https://doi.org/10.3390/xxxxx>
Published: 17 May 2023



Copyright: © 2023 by the authors. Submitted for possible open access publication under the terms and conditions of the Creative Commons Attribution (CC BY) license (<https://creativecommons.org/licenses/by/4.0/>).

1. Introduction

Mass transfer through hollow fiber membranes is a membrane-based separation process for gas mixtures and the removal of environmental pollutants, such as carbon dioxide. The difference between the partial pressures of the components is counted as one of the driving forces of mass transfer across the membrane. The hollow fiber membrane process is geometrically described as a solid, thick-walled, concentric anisotropic roll. A porous substrate and non-porous selective layers are the main distinct layers in this type of membrane [1]. The separation process is performed in the following steps: The initial feed of gas mixtures is contacted by the selective membrane surface. This mixture is in direct contact with the membrane surface, and the passing component is separated on the other side of the membrane. The vapor-phase substances passing through the membrane are called permeates, and the concentrated mixture coming from the feed stream is called retentate. Both retentate and permeate can be chosen as target products. The principle of separation of mixtures using hollow fiber membranes is presented in Figure 1.

The change in pressure can be indicated as the driving force for the membrane separation process. The substance in the initial raw mixture, the volume of which exceeds the pores of the membrane surface, is captured on the inlet side of the membrane and turns into a concentrated solution. The hollow fiber filtration is executed at ambient temperature and moderate pressure, which ensures low energy consumption. In addition, this type of process does not require heating or additional chemicals to achieve the purposes of separation, concentration, partition, cleaning, and classification. Fractions, colloids, bacteria, and macromolecular organics containing water can be effectively purified using membrane techniques [1].

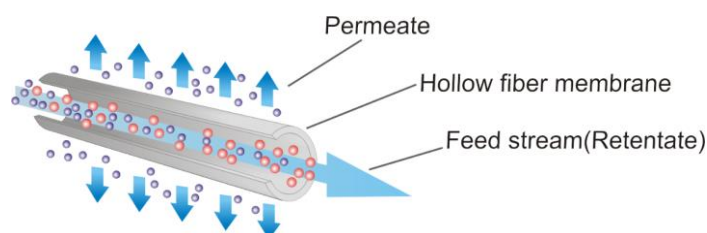


Figure 1. Principal scheme of the separation of a gas mixture using hollow fiber membrane.

Hollow fiber membrane process mechanisms involve various steps that must be closely monitored to ensure optimal performance. Initially, the fiber membrane is manufactured to have a porous structure with precise diameters and thicknesses, allowing for the separation of different substances [1].

It is crucial to maintain proper flow rates and pressures to optimize the separations. Fouling or clogging of the membrane can occur due to the deposition of impurities or organic materials, leading to reduced permeate flow and decreased efficiency. In such cases, cleaning protocols must be implemented to remove the accumulated materials and restore the productivity of the membrane. During the filtration process, the feed solution is passed through the interior of the hollow fibers, while a vacuum is applied outside the fibers to draw the permeate through the walls of the membrane. The retained and/or permeated components across the membrane are dictated according to the shape and dimension of the pores in the membrane [2].

2. Background

Accordingly, to the facilitated transport mechanism, the mixture is transferred from one boundary to the other in two various methods: the pure diffusion in the unreacted state and the diffusion in the form of complexes. Once on the underside of the membrane, the reverse reaction occurs and the mixture is released. Consequently, following to Fick's law the diffusion mechanism for each component, the resulting equation of total flux is the representation of the facilitated transport process [3].

$$J_i = - \left(D_A \frac{dC_A}{dx} + D_{AC} \frac{dC_{AC}}{dx} \right) \quad (1)$$

From the point of view of the facilitated transport, facilitation factor also has to be considered and it is a direct measure of the reaction effect on the transport. The facilitation factor can be calculated as the relation between the total flux of component i through the membrane in the x -direction, and the flux expressed by the pure diffusion mechanism:

$$F = \frac{D_A \frac{dC_A}{dx} + D_{AC} \frac{dC_{AC}}{dx}}{D_A \frac{dC_A}{dx}} \quad (2)$$

where, A—the mixture; C—the carrier; AC—the carrier complex species; D_A —the diffusivity of the mixture; C_A —the concentration of component A; D_{AC} —diffusion coefficient of AC; C_{AC} —concentration of AC.

The separation factor α is calculated using the concentrations of each component in two different phases. It is defined as the ratio of the equilibrium concentrations of the two components in the two phases:

$$\alpha_{i/j} = \frac{y_i/x_i}{y_j/x_j} \quad (3)$$

where y and x identify the gas content in the permeate and feed side, respectively.

In order to occur the permeation of component i predominantly, the separation factor must be higher than unity. If $\alpha = 1$, then both components have equal affinity for both phases and there is no separation preference. These compositions are described using mole, mass or volumetric fractions. The separation factor is an important parameter in designing separation processes such as distillation, liquid-liquid extraction, membrane processes and chromatography.

Another factor influencing the separation process is the pressure ratio (φ). This ratio helps to determine the efficiency of a membrane separation process by measuring the amount of pressure required to achieve the desired level of separation:

$$\varphi = \frac{p^{feed}}{p^{perm}} \quad (4)$$

where, p^{feed} and p^{perm} are the feed and permeate pressure respectively (in bar).

In the facilitated transport mechanism, the permeance of component i can be often expressed as following [3,4].

$$P_i = \frac{V_p(1 - y_j)y_i}{(\langle p_i^{feed}, p_i^{ret} \rangle - p_i^{perm})A} \quad (5)$$

where the total permeate flow V_p (ml s⁻¹) is measured experimentally. y_j and y_i are the molar fraction of the component j and permeating components i in the permeate side, respectively. p_i^{feed} , p_i^{ret} and p_i^{perm} partial pressures (cm Hg⁻¹) of the component i in the feed, retentate, and permeate, respectively. $\langle p_i^{feed}, p_i^{ret} \rangle$ is the average partial pressures of feed and retentate. Permeance is denoted in GPU, (GPU = 3.35 × 10⁻¹⁰ mol m⁻² s⁻¹ Pa⁻¹).

3. Modeling and Simulation of Membrane Process

Modeling and simulation are used in many purposes, including engineering, science, transportation economics and finance. They are used to investigate complex systems that are arduous or demanding to experiment in real process. These techniques use data from real-process experiments or observations to create models that can simulate the behavior of complex systems with high precision [5,6].

After considering the non-ideal gas behavior, the identification of the transport of component i through the membrane is defined by [7].

$$J_i = Q_i (p_i^0 x_i^{feed} \gamma_i - p_i^{perm}) \approx Q_i (\hat{f}_i^{feed} - \hat{f}_i^{perm}) \quad (6)$$

where \hat{f}_i^{feed} —the fugacity of component i in the feed stream; \hat{f}_i^{perm} —the fugacity of component i in the permeate side. The saturation vapor pressure (p_i^0) and the fugacity of components (\hat{f}_i) are obtained from the Antoine equation and Soave-Redlich-Kwong model, respectively. Q is a variable quantity depending on membrane surface area, thickness, and permeability. The average fugacity of components depends on the tentative parameters namely gas composition y_i , pressure P , and effect of real gas behavior φ_i on the both of the feed and permeate sides:

$$\hat{f}_i = \frac{P^{feed} \cdot y_i^{feed} \cdot \varphi_i^{feed} + P^{perm} \cdot y_i^{perm} \cdot \varphi_i^{perm}}{2} \quad (7)$$

In this work we have applied the experimental results for the carbon capture process by hollow fiber membrane accounted in the research conducted by Saravanan et al. [4] These experimental data have been combined into a model that describes the mass transfer across the membrane as a function of the fugacity of the components and conditions of experiments. Accordingly, Schuldt et al. (2018) the partial fluxes can be determined as a polynomial function of the fugacity of the species, which means that the permeance changes depending on this parameter [8] In summary, considering the different semi-empirical models described in references, we corrected the CO₂ permeability data to a justification that calculated depending on the fugacity of CO₂:

$$Q_{CO_2} = A_1 * (\hat{f}_{CO_2}^{perm})^2 + B_1 * \hat{f}_{CO_2}^{perm} + C \tag{8}$$

With regard to residue mixture, the permeance of this component can be described as a function of the fugacities of CO₂ and N₂:

$$Q_{ret} = A_2 * \hat{f}_{N_2}^{perm} + B_2 * \hat{f}_{CO_2}^{perm} + C_2 \tag{9}$$

We are assuming that only CO₂, N₂ permeate across the membrane surface, with the other components remaining on the retentate side of the substrate and not passing through. Using the ACM software, experimental permeation data from Saranan et al. [4] were fitted to Equations (5)–(8) to provide the predicted parameters listed in Table 1. Operating conditions are assumed to be at 1.7 bar supply pressure, 35 °C temperature and fully wet conditions.

Table 1. Model parameters for CO₂/N₂ mixtures permeating through hollow-fiber membrane.

Coefficients	Carbon Dioxide	Nitrogen
<i>A_i</i>	2.6 × 10 ⁴	30.9
<i>B_i</i>	7 × 10 ³	11.2
<i>C_i</i>	546.24	2.8
Fugacity at the feed	0.25	1.24

Figures 2 and 3 illustrate a comparison of experimental data [4] and model data fitting (Equations (5)–(8)).

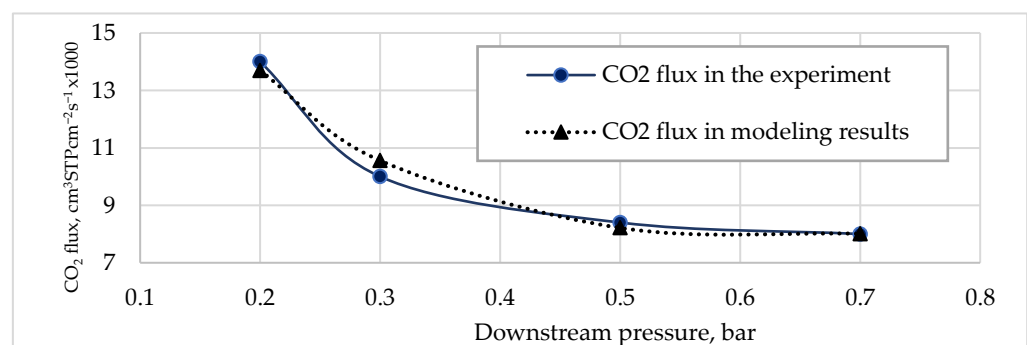


Figure 2. Pressure impact on the total flux across the membrane.

A mathematical model of a hollow-fiber membrane module was modified from Chu et al. (2019) and included the aforementioned membrane performance model in order to approximate the behavior of a hollow-fiber module at an industrial scale [9]. The following factors were considered while developing steady state mass and energy balances: (i) plug-flow for the inlet mixture, (ii) perfect mixing in the permeation, (iii) a minimal loss of temperature, (iv) minimal polarizing implications and (v) a slight pressure drop throughout the module. A discretization approach was used to divide the membrane module into a number of cells for computation reasons.

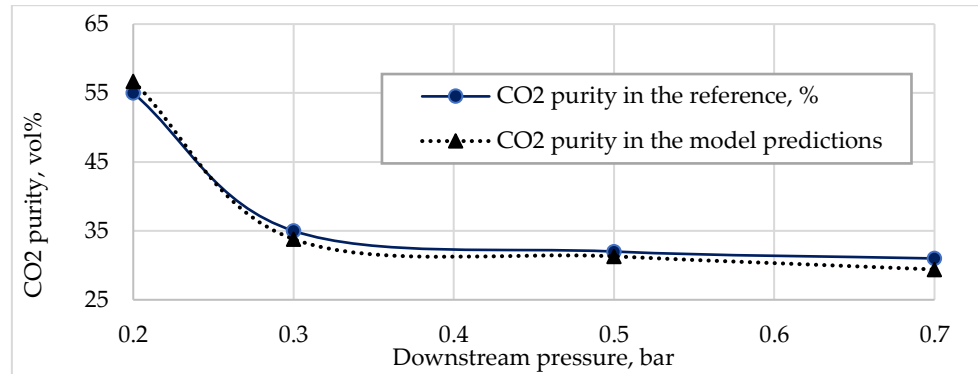


Figure 3. Influence of the pressure of permeate side on the CO₂ content in the permeate.

These results were obtained for an inlet flow pressure of 1.7 bar and a temperature of 30°C, but it was observed that the difference between these results increased depending on the inlet pressure was increased, and all other substances in permeate were assumed to be N₂.

Ordinary differential equations are used to express how composition and temperature of the retentate in each cell changes dynamically. The temperature on the retentate and permeate sides in each cell is considered to be the same because in general heat resistances through the membrane are insignificant. The total molar balance is algebraic since it is assumed that the molar holdup in each cell (M_R) is constant:

$$\frac{dM_R}{dt} = 0 = F_{R,n-1} - F_{R,n} - F_{P,n} \quad (10)$$

$$M_R \frac{dh_{R,n}}{dt} = 0 = F_{R,n-1}h_{R,n-1} - F_{R,n}h_{R,n} - F_{P,n}H_{P,n} \quad (11)$$

$$M_R \frac{dz_{R,n,i}}{dt} = 0 = F_{R,n-1}z_{R,n-1,i} - F_{R,n}z_{R,n,i} - F_{P,n}z_{P,n,i} \quad (12)$$

where $F_{R,n}$ —molar flowrate of the retentate from cell n (kmol h⁻¹); $F_{P,n}$ —molar flowrate of permeate from cell n (kmol h⁻¹); $h_{R,n}$ —molar enthalpy of retentate in cell n (GJ kmol⁻¹); $H_{P,n}$ —molar enthalpy of permeate leaving cell n (GJ kmol⁻¹); $z_{R,n,i}$ —molar fraction of component i in the retentate in cell n . $z_{P,n,i}$ —mole fraction of component i in the permeate leaving cell n . The permeate flowrate is calculated using the membrane area (A_{mem}) multiplied by the sum of the two component fluxes, and the permeate composition is determined by the partial flux to total flux ratio (Equation (13)):

$$F_{P,n} = A_{mem}(J_{n,CO2} + J_{n,N2}) \quad (13)$$

$$z_{P,n,i} = A_{mem} \times \frac{J_{n,i}}{F_{P,n}} \quad (14)$$

The flux of component i in each cell is calculated using the following equation:

$$J_i = Q_i(z_{Ri} \gamma_i P_i^{sat} - z_{Pi} P_{permeate}) \quad (15)$$

The retentate temperature is calculated from the determined enthalpy ($h_{R,n}$) and composition ($z_{R,n}$) of the retentate using physical characteristics of the medium [10].

4. Conclusions

The membrane process in this work is simulated using the ACM program. In order to calculate the composition and temperature of the retentate and permeate streams, the material and energy balances are simultaneously solved. To do this, the thermodynamic properties that are a function of pressure and composition need to be computed in each cell using subroutines specific in ACM software. Thus, properties such as fugacity, vapor

pressure, density, heat capacity, and liquid and vapor enthalpies are calculated as variables distributed along the membrane module. In addition, the membrane permeances are also calculated in each cell using the equations of the proposed model as a function of the fugacity of species and pressure. The differential and algebraic equations for each cell and each module are incorporated in the ACM program. In the case of study analyzed modules, the flux and purity of carbon dioxide in permeate side are approximately $700 \text{ NL m}^{-2}\text{h}^{-1}$ and 55 percent, respectively. These values are suitable for use in simulation purposes and the resulting flux corresponds to the experimental data. It was observed that the difference between these results increased depending on the inlet pressure was increased.

References

1. Sohail, S.; Ahmed, A.; Tanveer, H.U. Hollow Fiber Membrane for Filtration of Liquids. U.S. Patent 11148100B2, 1 May 2019.
2. Mourad, L.; Antonio, S.J.; Khayet, M.; García-Payo, C.; Chaouch, M. Fouling in Membrane Distillation, Osmotic Distillation and Osmotic Membrane Distillation. *Appl. Sci.* **2017**, *7*, 334. <https://doi.org/10.3390/app>.
3. Rea, R.; De Angelis, M.G.; Baschetti, M.G. Models for Facilitated Transport Membranes: A Review. *Membranes* **2019**, *9*, 26. <https://doi.org/10.3390/membranes9020026>.
4. Saravanan, J.; Santinelli, F.; Costi, R.; Lindbråthen, A.; Nardelli, G.M.; Milkowski, K.; Ansaloni, L.; Deng, L. Field trial of hollow fiber modules of hybrid facilitated transport membranes for flue gas CO₂ capture in cement industry. *Chem. Eng. J.* **2021**, *413*, 127405.
5. Lipnizki, F.; Trägårdh, G. Modelling of pervaporation: Models to analyze and predict the mass transport in pervaporation. *Sep. Purif. Methods* **2001**, *30*, 125–149.
6. Norkobilov, A. Design of Hybrid Separation Processes Incorporating Membrane Technologies. Thesis, Universidad de Cantabria, Santander, Spain, 2017.
7. Miandoab, E.S. Effective Modelling of Industrial Scale Membrane Gas Separation Processes, Thesis, The University of Melbourne, Melbourne, Australia, 2021.
8. Schuldt, K.; Pohlmann, J.; Shishatskiy, S.; Brinkmann, T. Applicability of PolyActive™ Thin Film Composite Membranes for CO₂ Separation from C₂H₄ Containing Multi-Component Gas Mixtures at Pressures up to 30 Bar. *Membranes* **2018**, *8*, 27. <https://doi.org/10.3390/membranes8020027>.
9. Chu, Y.; Lindbråthen, A.; Lei, L.; He, X.; Hillestad, M. Mathematical modeling and process parametric study of CO₂ removal from natural gas by hollow fiber membranes. *Chem. Eng. Res. Des.* **2019**, *148*, 45–55. <https://doi.org/10.1016/j.cherd.2019.05.054>.
10. Gorri, D.; Norkobilov, A.; Ortiz, I. Optimal Production of Ethyl Tert-butyl Ether using Pervaporation-based Hybrid Processes through the Analysis of Process Flowsheet. *Comput. Aided Chem. Eng.* **2017**, *40*, 1123–1128. <https://doi.org/10.1016/B978-0-444-63965-3.50189-6>.

Disclaimer/Publisher's Note: The statements, opinions and data contained in all publications are solely those of the individual author(s) and contributor(s) and not of MDPI and/or the editor(s). MDPI and/or the editor(s) disclaim responsibility for any injury to people or property resulting from any ideas, methods, instructions or products referred to in the content.